Experimental Study on Transmission of Visible Light in Table Salt Water and Effect on Underwater Wireless Optical Communication

Oluwabukola A. Ojediran, Akinlolu A. Ponnle, and Samson A. Oyetunji

***Abstract* — Underwater wireless optical communication (UWOC) has advantages over other underwater communication methods. Some of these advantages are high data rates, large bandwidth, and less susceptibility to electromagnetic interference. The transmission of light underwater is affected by absorption, scattering and turbulence. Sodium Chloride is one of the most abundant dissolved substances in seawater which cause attenuation of optical signals. In this work, the effect of table salt in water on transmission of visible light in the range 400nm – 800nm was investigated. Nine samples of 100 ml of pure water were prepared in which eight of the samples contain addition of table salt of 1g, 3g, 4.5g, 5.5g, 15g, 20g, 25g and 28g yielding different salt concentrations (salinity). The conductivity, total dissolved solids (TDS), and total dissolved salt of the samples were measured. Absorption spectra of visible light through these samples were obtained using a spectrophotometer. The results showed an increase in conductivity and attenuation with increase in the presence of the table salt in the water. Also, it was observed that at shorter wavelengths (blue light), there is higher attenuation with increase in salt concentration compared to longer wavelengths (red light). However, the attenuation tends to increase sharply around 700nm – 800nm. From the absorption spectra obtained for each sample, the absorptivity spectrum for the table salt was obtained which shows high absorptivity at shorter wavelengths and lower absorptivity at longer wavelengths. From the absorption coefficient values obtained from the measurements, performance of UWOC for selected samples at three wavelengths of 450nm, 550nm and 700nm with transmitter power of 30mW were evaluated by simulation using OptiSystem linked with MATLAB. For a maximum allowable Bit Error Rate (BER) of 10^{-9} in UWOC, achievable link distance reduces considerably as the salt concentration increases.**

***Key words* — absorbance; attenuation; bit error rate; salinity; underwater wireless optical communication.**

I. INTRODUCTION

Underwater communication has applications in many areas such as in oceanography research, surveillance, fish tracing, offshore explorations, oil control and maintenance, climatic change monitoring, and ecological changes. There is increase in the number of vehicles and devices deployed underwater that need high bandwidth to send information underwater [1]. The underwater environment encompasses about two-thirds of the earth's surface [2]. The technologies used for underwater communication are acoustic, optical, fiber and radio frequency waves.

Underwater wireless optical communication (UWOC) provides high bandwidth, high data rates, lower power consumption, flexibility, better security, less susceptibility to electromagnetic interference, and lower cost than the other methods, though at shorter distances. The blue-green (450-570 nm) wavelength is preferred for transmission in pure seawater since there is less attenuation at these wavelengths. However, the optical window shifts to longer wavelengths when suspended particles are present. The effects of absorption, scattering and turbulence on optical waves cause attenuation that limits its propagation to short distances.

Pegau *et al.* [3] obtained the absorption coefficient of pure and saline water in the visible and near-infrared parts of the electromagnetic spectrum. The absorption coefficient depended on temperature in the near-infrared region while it was less for the visible portion.

Al-Azzawi *et al.* [4] investigated the optical property of tap water through the addition of measured concentrations of sodium chloride and clay to the medium. A spectrophotometer determined the transmittance and absorbance at different lengths. The transmitted intensity decreases while absorbance increases with increase in distance.

Li *et al.* [5] experimentally determined the optical properties of sodium chloride solution with concentration of (0-360 g/L) and wavelength (300–2500 nm). The results showed a non-linear increase in the refractive index of the saline water with respect to the salt concentration. In the visible light region, the absorption index of the salty water increases as the salt concentration increases. However, there is a minimal difference in the near infra-red portion (700–2500 nm).

Han *et al.* [6] observed the effect of absorption of inorganic salt concentrations of Sodium Chloride, Magnesium Chloride, Potassium Chloride, Sodium Bicarbonate, and Magnesium Sulphate using a UV (Ultraviolet)-spectrophotometer. The absorption of the saline water was scanned from 200–1200 nm, and the lowest attenuation was between 450–633 nm. An increase in concentration of the salts increases the attenuation.

Mohammad *et al.* [7] developed a communication channel using fresh and salty water with and without air bubbles. The effect of salt and air bubbles on underwater channel was shown that salt attenuates received signal and air bubbles introduce intensity fluctuations.

Submitted on March 01, 2022.
Published on March 22, 2022.
O. A. Ojediran, Federal University of Technology, Akure, Nigeria. (corresponding e-mail: bukiojed@gmail.com)
A. A. Ponnle, Federal University of Technology, Akure, Nigeria. (e-mail: ponnleakinlolu@yahoo.co.uk)
S. A. Oyetunji, Federal University of Technology, Akure, Nigeria. (e-mail: saoyetunji@futa.edu.ng).

Matthew *et al.* [8] developed an underwater optical communication system using white LED and a 650nm red laser diode as transmitters and a PIN photodiode as a receiver. The LEDs gave good reception at transmitter to receiver distance between 5-15 cm for clear water and 5-10 cm for saline water.

Kumar *et al.* [9] studied the effect of salinity on UWOC by utilizing different salt concentrations in an experimental setup. A mathematical model was used to evaluate the saline water with the experimental data. The simulation was done in OptiSystem linked with MATLAB software for different data rates and link lengths. The attenuation increased as the salinity increased; and the performance of the system reduced at higher data rates and longer link length.

Adnan *et al.* [10] experimentally transmitted texts using pulse width modulation in an UWOC channel that contained different values of salinity formed from various concentrations of sodium chloride. The results of the experiment depict the attenuation coefficient to be low in water of low salt concentration, which is consistent with pure seawater, while the attenuation coefficient is high in water of high salt concentration which is consistent with turbid harbor water.

Elamassie *et al.* [11] utilized a transmitter with multiple laser sources and one receiver to reduce the effects of salinity fluctuations underwater.

Elamassie *et al.* [12] modelled the vertical underwater link to show how the salinity changes with depth. The models were used to derive expressions for the BER performance of the links. In a vertical UVLC link, water with different values of salinity form non-mixing layers due to ocean stratification. This results in variations of turbulence strength through the transmission range.

In this work, attenuation effect of common unfiltered table salt of varying concentration on performance of underwater optical communication within the visible light range was investigated. Absorption spectra were obtained using a spectrophotometer, from which the variation of the absorption with salt concentration, and absorptivity spectrum was investigated. Attenuation at three different wavelengths was then used to evaluate the performance of UWOC by simulation.

II. Optical Properties of Water and UWOC Performance

A. Optical Properties of Water

Water is transparent because it has very low absorption in the visible light region [13]. The transmission of light underwater is wavelength selective because different types of water have different spectral properties of absorption [14]. The attenuation of electromagnetic wave in pure water within the wavelength of 40 nm and 600 μm is shown in Fig. 1 [15]. The blue–green wavelengths (420–532 nm) give a low attenuation window as discovered by Sullivan and Dimtle in 1963 (reported in [6]), and the attenuation increases gradually towards the red wavelengths. This makes it possible for underwater communication in the visible light range.

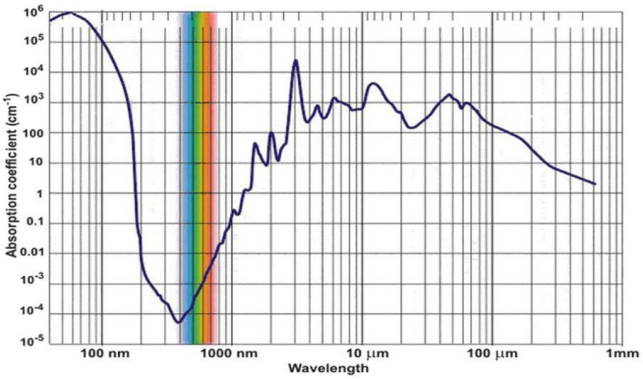

Fig. 1. Optical window of attenuation of e.m. wave in pure water [15].

Seawater is composed of organic, inorganic, dissolved and suspended materials. It consists of mineral elements like iodine and boron. Table salt is obtained when seawater is evaporated. In pure sea water, absorption is the major limiting factor [16]. The deep clear ocean is blue in colour because the red wavelength is more attenuated than the blue wavelength. Clear ocean water has a higher concentration of salts, mineral components, organic matter, and other dissolved particles that cause large amount of scattering.

B. Water Structure and Absorption in Water

Absorption is the irreversible loss of intensity, and it depends on the refractive index of water [17] and the spectral absorption coefficient. The major cause of light absorption in water is the excitation of the state of the water molecule and other dissolved particles when photons of a light wave collide with them [18]. Each photon losses energy thermally [19], and the energy lost is converted into other forms such as heat, chemical, etc. [20].

The water molecule is composed of two hydrogen atoms and one oxygen atom. The presence of lone-pair electrons in the outer shell of the oxygen atom results in a non-linear structure along the H-O-H bond. There are three types of vibrations and librations (swaying back and forth of the molecules) in three axes due to the non-linear structure of the water molecule. The three vibrations are symmetric stretching, bending, and asymmetric stretching. The main absorption bands of liquid water in the infrared range of the electromagnetic spectrum are due to these three vibrations.

The bending results in absorption near infrared with harmonics extending down to the visible light range. The stretching absorption bands occur around far infrared with harmonics in the visible light range. The stretching and bending vibrations are also affected by pressure, temperature and contaminants in the water. An increase in temperature reduces the strength of the hydrogen bonds, the stretching vibrations shifts to higher frequencies and the bending vibrations to lower frequencies [13].

C. Scattering

Scattering is the change of the path of the light beam from its original path due to suspended particles but with no change in energy [21]. The particles might be of comparable size to the wavelength in water (diffraction) or particles whose refractive index varies from that of water (refraction) [20]. The light is dispersed into many directions and results in loss of light intensity at the receiver.

D. Salinity

Salinity is the amount of dissolved salt in water. It is measured in kilogram of salt per kilogram of water or in parts per thousand (ppt). Salinity can be measured by measuring the dissolved salts in a solution or by electrical conductivity as there is a direct relationship between electrical conductivity and salinity.

Total dissolved solid (TDS) is a measure of the dissolved content of all organic and inorganic substances present in a liquid. TDS is usually measured in parts per million (ppm), it can also be indicated in parts per thousand (ppt).

Salinity of some rivers in Nigeria are: Osun river: 0.06-0.17 ppt [22]; Imo river: 12.66 ppt [23]; Escravos: 15 ppt [24]; Bonny river: 15.33-15.50 ppt [25]; and Nkoro river: 12.88 ppt [26]. The average salinity of seawater is about 33-38 ppt.

E. UWOC Performance

The optical properties of water are used for modeling the underwater channel. These properties are inherent and apparent properties. Inherent property depends on the water medium such as absorption and scattering while apparent property depends on the medium and the directional properties of the ambient light field.

In UWOC, Beer Lambert's law gives the transmitted optical power as a function of distance and attenuation in the medium which is wavelength dependent as in (1):

$$P(x,\lambda) = P_o e^{-c(\lambda)x} \quad (1)$$

where P_o is the initial optical power from the transmitter, and $P(x,\lambda)$ is the transmitted optical power through the medium at distance x, and $c(\lambda)$ is the attenuation coefficient. The attenuation coefficient $c(\lambda)$, comprises of absorption coefficient, $a(\lambda)$ and scattering coefficient $b(\lambda)$, as expressed in (2).

$$c(\lambda) = a(\lambda) + b(\lambda) \quad (2)$$

Also from Beer's law, Absorbance (A),

$$A = \varepsilon l m \quad (3)$$

where ε is the molar absorptivity, l is the path length, and m is the concentration. Equation (3) shows that absorbance is directly proportional to concentration. It is also wavelength dependent, and because of this, the molar absorptivity is also wavelength dependent.

If I_o is the intensity of light as it enters a sample, and I is the intensity of light as it leaves the sample to the photo detector, then I and I_o are related by:

$$I = I_o\left(10^{-\varepsilon(\lambda)lm}\right) \quad (4)$$

from which Absorbance,

$$A(\lambda) = -\log_{10}\left(\frac{I}{I_o}\right) \quad (5)$$

Absorption coefficient can be obtained from absorbance as in (6):

$$\alpha(\lambda) = 2.3026A(\lambda) \quad (6)$$

The absorption coefficient is expressed as the fraction of the absorbed energy from a beam of light per unit of distance travelled in an absorbing medium [27]. Absorption coefficient is measured in cm^{-1} or m^{-1}.

III. Materials And Methods

A. Measurement of Salinity

The following ingredients are contained in the table salt used to prepare the samples: common salt, iodine (50 ppm) and potassium/sodium ferrocyanide (anti-caking agent, 10 ppm). Salt weights of 1 g, 3 g, 4.5 g, 5.5 g, 15 g, 20 g, 25 g and 28 g were dissolved in 100ml of pure water. Seawater concentration corresponds to salt weights of about 3.5 g/100 ml. The electronic balance (model FA2104A) was used to weigh the salts. The electrical conductivity, temperature, total dissolved solids (TDS), and total dissolved salt of each salt solution were measured with the aid of a water quality tester EZ-9909SP.

B. Absorbance Measurement

A VIS-721 Visible Light Spectrophotometer was used (shown in Fig. 2) to determine the absorption spectra of the salt solutions in the visible light range. The measurement of each sample was done with a pipette and placed in a cuvette of length of 10 mm. The cuvette was cleaned with distilled water prior to each scan to prevent contamination by other solutes. An empty cuvette was used as the reference and the salt water samples were placed in the sample cuvette. The scan of the absorption spectrum of the different samples were obtained with respect to the wavelengths in the range 400–800 nm, and recorded. The measurements were made at wavelength intervals of 50 nm. From the spectra obtained, average absorption for each sample was evaluated, as well as the absorptivity at different wavelengths.

Fig. 2. The VIS-721 Visible Spectrophotometer.

C. UWOC Simulation

Using the absorption coefficients evaluated for selected samples of 1 g, 3 g, 5.5 g, 20 g and 28 g per 100 ml of pure water, UWOC for each sample with a continuous laser beam

of 30 mW at 450 nm, 550 nm, 700 nm and data rate of 10Gb/s was simulated using OptiSystem software linked with MATLAB. The performance was evaluated in terms of maximum link distance achievable for the maximum allowable BER in UWOC of 10^{-9} [28]. The Quality Factor (QF) was also determined. The schematic layout of the UWOC in OptiSystem is shown in Fig. 3, and the simulation parameters are shown in Table I.

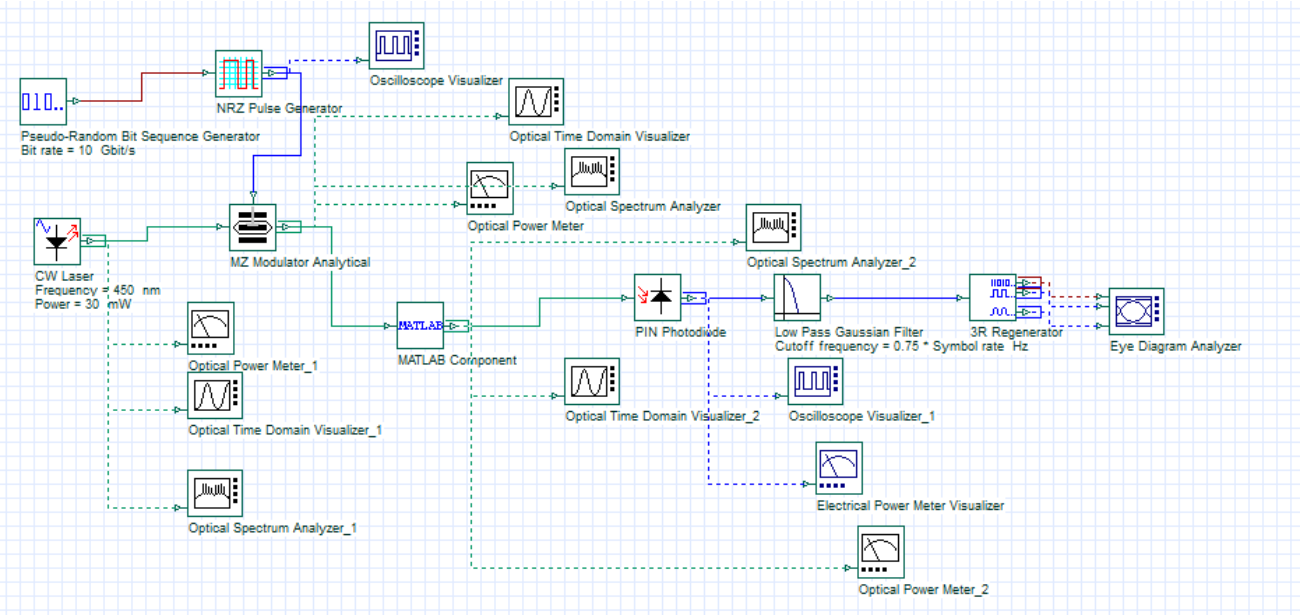

Fig. 3. Schematic layout of the UWOC in OptiSystem.

TABLE I: SIMULATION PARAMETERS

Parameters	Values
Operating Wavelength of Laser	450 nm, 550 nm, 700 nm
Power of Laser	30 mW
Bit rate of bit sequence generator	10 Gbps
Modulation	NRZ OOK
Amplitude of NRZ pulse generator	1 a.u.
Responsivity of Photodetector	1 A/W
Dark current of Photodetector	10 nA
Cutoff frequency of filter	0.75 × Bit rate

The pseudorandom bit sequence generator (PRBS) generates a pseudo random binary sequence at a bit rate of 10 Gbps. The Non-Return to Zero (NRZ) pulse generator receives the binary signal from the PRBS and produces a sequence of rectangular NRZ electrical pulses coded by the input PRBS signal.

The continuous wave (CW) Laser produces a continuous wave laser beam (optical signal) at determined wavelengths and power. The Mach Zender (MZ) Modulator receives an electrical input from the NRZ and use the CW laser to produce a modulated optical output.

The MATLAB Component represents the underwater channel. It receives the optical signal from the MZ modulator and produces an optical signal that is attenuated. It runs the MATLAB code that is linked with the Optisystem.

The Pin Photodiode receives the attenuated optical signal and gives an electrical output signal based on the receiver's responsivity. The low pass Gaussian filter is a filter with a Gaussian frequency transfer function that is used to reduce noise.

The 3R regenerator receives electrical input from the low pass filter and produces binary, electrical reference signal and electrical signal outputs which are passed to the Eye Diagram Analyzer. The eye diagram analyzer shows the electrical signals in the shape of an eye. The Q factor, BER, eye height and threshold can be determined from the eye diagram.

IV. RESULTS AND DISCUSSION

A. *Measurement of Salinity*

Table II shows the measured parameters of the table salt water samples. From the Table II, it can be observed that the electrical conductivity of the water samples increases as more salt is added to the water. The total dissolved solids and temperature of the water also increases with increase in salt concentration. The table also reveals that as more salt is added to the water samples, more other dissolved solids are added. The values of the TDS indicated contain both the total dissolved salt and some other dissolved solids.

TABLE II: MEASURED PARAMETERS OF THE SALT WATER SAMPLES

Weight of salt (g) in 100 ml of pure water	Electrical Conductivity (mS/cm)	Temperature (°C)	Total Dissolved Salt (ppt)	TDS (ppt)
Pure Water	0.002	24.80	0.001	0.001
1.0	17.76	25.00	8.85	9.86
3.0	58.70	25.10	29.30	36.10
4.5	83.70	25.20	41.80	52.80
5.5	96.10	25.30	48.20	62.00
15.0	196.80	25.40	97.30	147.80
20.0	223.20	25.50	111.60	170.50
25.0	243.00	26.50	121.50	187.10
28.0	248.00	26.70	124.00	192.00

Fig. 4 shows how the electrical conductivity of the salt water samples increases with addition of the table salt into the water. It increases linearly initially with increase in quantity of salt added, but after some values it tends to slowly increase with more quantity of the table salt. Fig. 5 shows how the total dissolved salt and the resulting total dissolved solids (both measured in ppt) vary with quantity of

salt added. They both show similar pattern as that of the electrical conductivity. At higher quantities of added table salt by weight, the measured total dissolved salt in ppt slowly increases. Fig. 6 shows how the water electrical conductivity varies with total dissolved salt and total dissolved solids (both in ppt). The variation of conductivity of the water with total dissolved salt and total dissolved solids can be seen to be both linear, but perfectly linear with total dissolved salt. This shows that the total dissolved salt contributes mostly to the electrical conductivity of the table salt water.

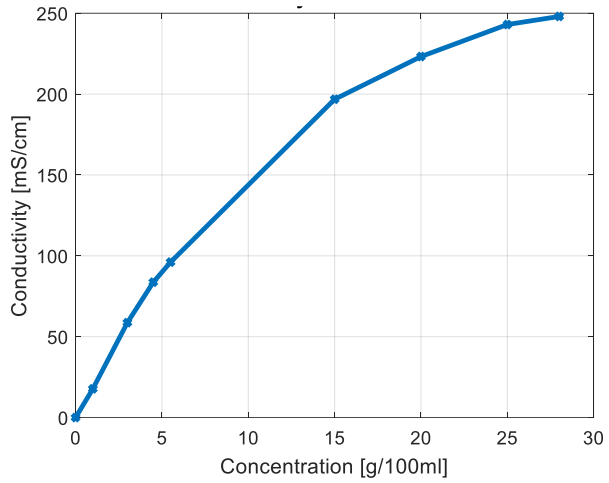

Fig. 4. Electrical conductivity of the water samples with salt concentration.

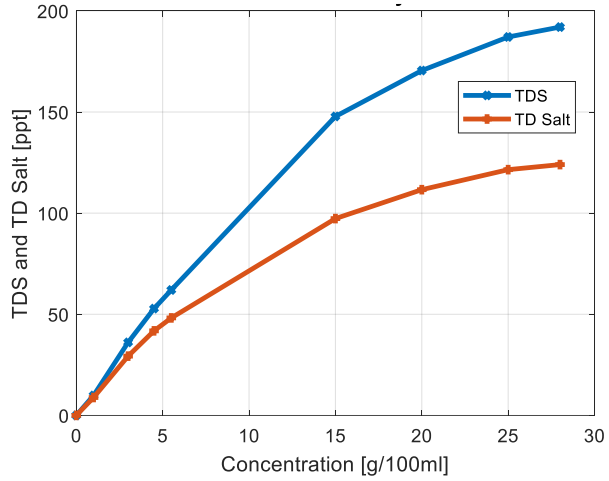

Fig. 5. Total dissolved solid and total dissolved salt with salt concentration.

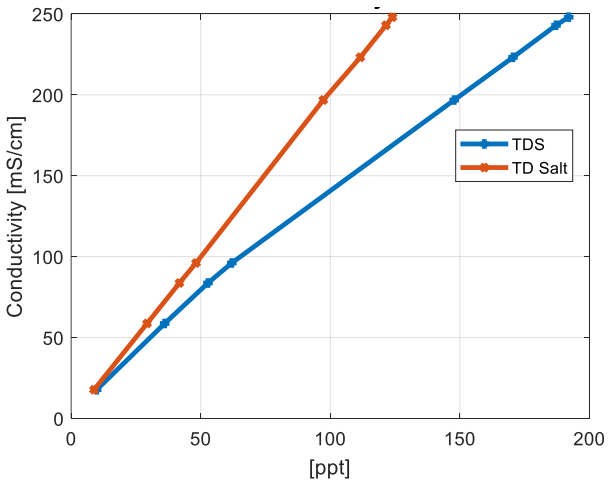

Fig. 6. Electrical conductivity with TDS and total dissolved salt.

B. *Absorption Measurement*

The results of absorption measurements within visible wavelengths of 400–800nm for the eight samples are shown in Fig. 7. As salt is added to the water at 1 g/100 ml concentration and with higher salt concentrations of the samples, there is more attenuation at the shorter wavelengths (400–450 nm) than at the longer wavelengths (650–700 nm). Between 700-750 nm (towards infra-red), the absorbance increases sharply while there is a reduction in the absorbance between 750-800 nm (infra-red).

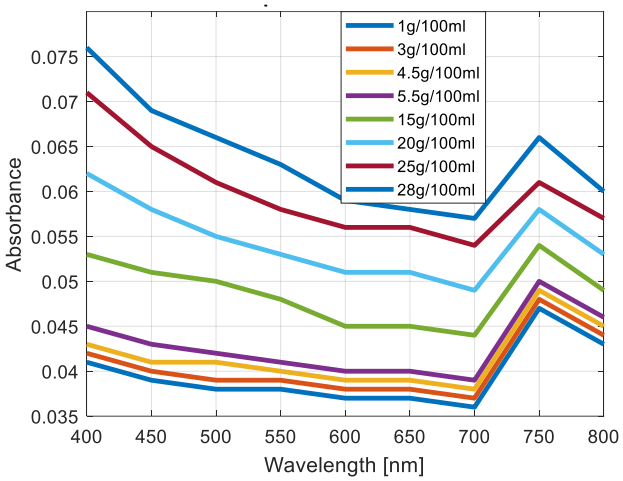

Fig. 7. Plot of the absorbance of different concentrations of the salty water between 400–800 nm.

Fig. 8 shows the average absorption (over the entire visible light range) of each sample with salt concentration and the water electrical conductivity respectively.

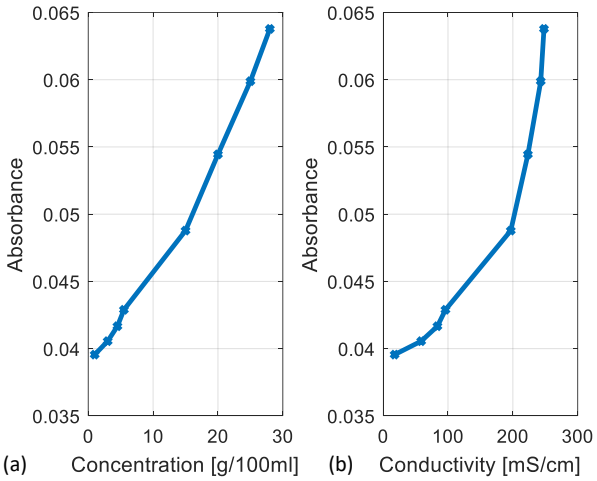

Fig. 8. Average absorption with (a) salt concentration, and (b) electrical conductivity.

It can be observed that the average absorbance increases with salt concentration, as well as with the water electrical conductivity. A linear relationship between the absorbance and salt concentration can be observed. This agrees with literature. Same is observed with the water electrical conductivity though the linearity is less obvious. Nevertheless, absorbance increases as the conductivity due to salinity increases.

Careful observation of Fig. 7 shows that as the salt concentration is increased, higher values of attenuation are obtained at shorter wavelengths than at longer wavelengths

(till 700 nm). This is depicted in Fig. 9 which shows the absorption with salt concentration at specific wavelengths of 450 nm, 550 nm, and 700 nm. In the figure, it can be observed that the rate of increase of absorption with concentration is highest at 450 nm and is least at 700 nm.

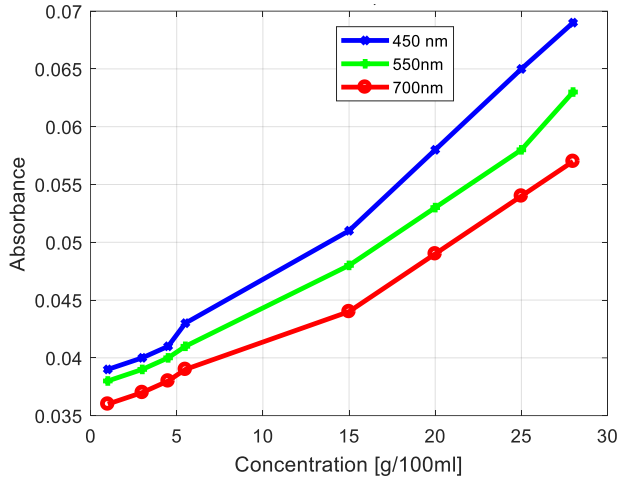

Fig. 9. Absorption at 450 nm, 550 nm and 700 nm with salt concentration.

Applying curve fitting (in MATLAB) to each plot at every wavelength of measurement in order to obtain model equation at each of the wavelength, the slope of the resulting straight-line equation model gives the rate of increase of absorbance with concentration at each of the wavelength. The fitted curves are linear polynomial model of order 1, having a general form expressed in (7):

$$f(x) = p_1 x + p_2 \tag{7}$$

where *f(x)* is the absorbance A, *x* is the concentration *m*, p_1 is the slope (which is the absorptivity, ε), and p_2 is the y - intercept.

From the curve fitting, values of slope were obtained for all the wavelengths, and Fig. 10 shows the absorptivity obtained at different wavelengths for the table salt water. The absorptivity is highest at 400 nm (blue light) and reduces gradually towards the longer wavelengths (red light and infra-red).

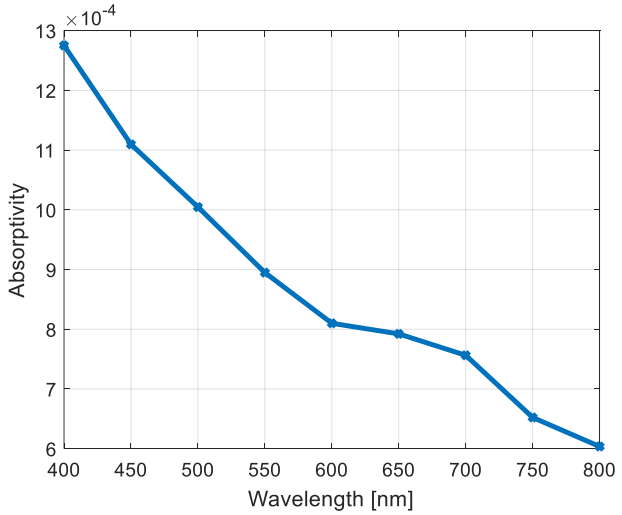

Fig. 10. Absorptivity of the table salt water between 400nm - 800nm.

Therefore, it can be inferred from this result that the range of visible light wavelengths that give the least attenuation in pure water would also give the highest attenuation when common table salt is introduced, and salinity of the water is increased. Since scattering is more pronounced at shorter wavelengths than longer wavelengths, therefore, the observed increased attenuation has to be due to higher absorption and scattering loss because of the increased dissolved salts, dissolved solids, and other particles introduced into the water with increased concentration.

C. UWOC Simulation and Performance

Results of the simulation in terms of maximum link distance achievable for the maximum allowable BER in UWOC of 10^{-9} at 450 nm, 550 nm and 700 nm for the selected samples of concentrations are shown in Fig. 11. Table III shows the BER and QF obtained from the simulation yielding the distances indicated.

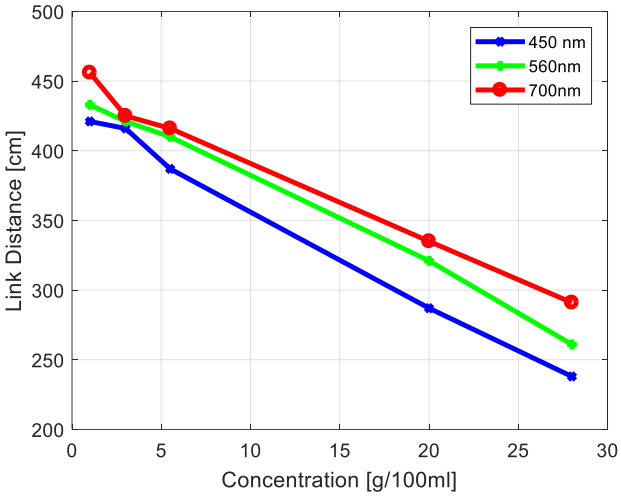

Fig. 11. Maximum link distance achievable for the maximum allowable BER.

TABLE III: RESULTS OF SIMULATION FOR BER OF 10^{-9} AT 450 NM, 550 NM AND 700 NM

Wavelength (nm)	Water Sample (g/100ml)	BER	Quality Factor
450	1	1.14×10^{-9}	5.98
	3	3.54×10^{-9}	5.79
	5.5	4.85×10^{-9}	5.74
	20	3.17×10^{-9}	5.81
	28	4.02×10^{-9}	5.77
550	1	5.49×10^{-9}	5.72
	3	1.76×10^{-9}	5.90
	5.5	1.93×10^{-9}	5.89
	20	1.59×10^{-9}	5.92
	28	1.33×10^{-9}	5.95
700	1	1.43×10^{-9}	5.94
	3	1.97×10^{-9}	5.89
	5.5	1.95×10^{-9}	5.89
	20	3.66×10^{-9}	5.78
	28	5.79×10^{-9}	5.71

It can be observed from Fig. 11 that for the simulation parameters used, and for a maximum allowable BER of 10^{-9} in UWOC, link distance of 456 cm is achievable for the 1 g/100 ml concentration at 700 nm, while the link distance reduces considerably as the salinity increases for the 3 wavelengths. The least distance is at 450 nm while the greatest distance is at 700 nm for all the salt concentrations.

Since same BER was targeted in the simulations, therefore the obtained QFs (in Table III) are closely similar for all.

V. Conclusion

This paper investigated the transmission of visible light (in the range 400-800 nm) in table salt water via spectroscopy, and its attenuation effect on underwater wireless optical communication. The absorbance of pure water is reduced in the blue-green wavelength however, as the salinity is increased, the absorbance of the blue light increases at a higher rate than the red light. The effects of absorption with salt concentrations are more pronounced at shorter wavelengths when compared to longer wavelengths. The absorptivity shows similar trend with wavelength.

Underwater wireless optical communication setup simulation shows that at any transmission wavelength, the link distance reduces as the salinity increases. Also in salty water, longer link distance is possible with longer wavelengths than with shorter wavelengths.

The results obtained from the measurements and simulations from this work can be used in the setup of underwater simultaneous multi-colour optical wireless communication systems to improve UWOC in salty water.

Acknowledgment

The authors thank the Department of Electrical and Electronics Engineering, Federal University of Technology Akure, Nigeria for providing some of the facilities for the experimental study.

Conflict of Interest

The authors declare that there is no conflict of interest.

References

[1] Kaushal H, Kaddoum G. Underwater Optical Wireless Communication. *IEEE Access*, 2016; 5: 1518-1547.

[2] Shen C, Guo Y, Oubei HM, Ng TK, Liu G, Park K, Ho K, Alouini M, Ooi BS. 20 meter underwater wireless optical communication link with 1.5 Gbps data rate. *Optical Society of America*, 2016); 24(22): 25502-25509.

[3] Pegau W, Gray D, Zaneveld J. Absorption and attenuation of visible and near-infrared light in water: dependence on temperature and salinity. *Optical Society of America, Applied Optics*, 1997; 36(24): 6035-6046.

[4] Al-Azzawi Z, Abdulzahra N, Hammood I. Optical properties of tap-water purity using He-Ne laser with different power density. *Journal of Al-Nahrain University*, 2014; 17(3): 99-107.

[5] Li X, Liu L, Zhao J, Tan J. Optical properties of NaCl solution within the spectral range from 300nm to 2500nm at room temperature. *Society for Applied Spectroscopy*, 2015; 69(5): 635-640.

[6] Han X, Peng Y, Zhang Y, Ma Z, Wang J. Research on the attenuation characteristics of some inorganic salts in seawater. *Journal of the European Optical Society Rapid Publications*, 2015; 10: 15045-1-15045-5.

[7] Mohammad VJ, Pirazh K, Arvin T, Ata C. Statistical Distribution of Intensity Fluctuations for Underwater Wireless Optical Channels in the Presence of Air Bubbles. *IEEE Iran Workshop on Communication and Information Theory*, pp. 1-6, 2016.

[8] Matthew L, Singh YP, Sharma S. An Extensive Study on Under-water Communication using LED /LASER Enabled Li-Fi Modules. *International Journal of Innovative Research in Science Engineering and Technology*, 2016; 5(11): 19435-19440.

[9] Kumar S, Prince S, Aravind JV, Kumar SG. Analysis on the effect of salinity in underwater wireless optical communication. *Marine Geo-resources and Geo-technology, Taylor & Francis Group*, 2019; pp.1-11. Doi: 10.1080/1064119X.2019.1569739.

[10] Adnan S, Hassan H, Alchlaby A, Kadhim A. Experimental study of underwater wireless optical communication from clean water to turbid harbour water under various conditions. *International Journal of Design, Nature and Eco-dynamics* (*IJDNE*), 2021; 16(2): 219-226.

[11] Elamassie M, Al-Nahhal, M, Kizilirmak, RC, Murat Uysal. Transmit Laser Selection for Underwater Visible Light Communication Systems. *IEEE 30th Annual International Smposium on Personal Indoor and Mobile Radio Communications*, pp. 1-6, 2019.

[12] Elamassie M, Uysal M. Vertical Underwater Visible Light Communication Links. *IEEE Transactions on Wireless Communications*, 2020; 19(10): 6948-6959.

[13] Peters R. Using spectra measurements to differentiate between aqueous NaCl and aqueous KCl in dual salt-solutions. Master's Thesis in the Department of Chemical and Biological Engineering, University of Saskatchewan, Saskatoon, 2016.

[14] Anguita D, Brizzolara D, Parodi G. VHDL Modules and Circuits for Underwater Optical Wireless Communication Systems. *WSEAS Transactions on Communications*, 2010; 9(9): 525-552.

[15] Zeng Z, Zhang H, Dong Y, Cheng J. A Survey of Underwater Wireless Optical Communication. *IEEE Communications Surveys and Tutorials*, 2016; 19(1): 1-62.

[16] Gabriel C, Khalighi M, Bourennane S, Leon P, Rigaud V. Investigation of Suitable Modulation Techniques for Underwater Wireless Optical Communication. *International Workshop on Optical Wireless Communications*, pp. 1-3, 2012.

[17] Gabriel C, Khalighi M, Bourennane S, Leon P, Rigaud V. Monte-Carlo-Based Channel Characterization for Underwater Optical Communication Systems. *Optical Communication Networks*, 2013; 5(1): 1-12.

[18] Sui M, Yu X, Zhang F. The Evaluation of Modulation Techniques for Underwater Wireless Optical Communications. *International Conference on Communication Software and Networks*, pp. 138-142, 2009.

[19] Jamali VM, Khorramshahi P, Tashakori A, Chizari A, Shahsavari S, AbdollahRamezani S, Fazelian M, Bahrani S, Salehi AJ. Statistical Distribution of Intensity Fluctuations for Underwater Wireless Optical Channels in the Presence of Air Bubbles. *IEEE Iran Workshop on Communication and Information Theory*, pp. 1-6, 2016.

[20] Elamassie M, Miramirkhani F, Uysal M. Channel Modeling and Performance Characterization of Underwater Visible Light Communications. *IEEE International Conference on Communication Workshops*, pp. 1-5, 2018.

[21] Jasman F, Green JR. Monte Carlo Simulation for Underwater Wireless Communications. *International Workshop on Optical Wireless Communications*, pp. 113-117, 2013.

[22] Anifowose AJ, Oyebode AW. Studies on heavy metals contents of Osun River at the pre-urban settlement and across Osogbo City, Nigeria. *Journal of Taibah University for Science*, 2019; 13(1): 318-323.

[23] Essien AL, Ofor CO. The physico-chemical characteristics of Imo River Estuary in southeastern Nigeria. *Tropical Freshwater Biology*, 2012; 21(1): 27-35.

[24] Ukpe ET, Ajayi TO. Marine fishery resources of Nigeria; a review of exploited fish stocks. Food and Agriculture Organization of the United Nations, pp.40-41, 1986.

[25] Onojake MC, Sikoki FD, Omokheyeke O, Akpiri RU. Surface water characteristics and trace metals level of the Bonny/New Calabar River estuary, Niger Delta, Nigeria. *Applied Water Science*, 2017; 7(2), 951-959. https://doi.org/10.1007/s13201-015-0306-y.

[26] Abowei J. Salinity, dissolved Oxygen, pH and surface water temperature conditions in Nkoro River, Niger Delta, Nigeria. *Advance Journal of Food Science and Technology*, 2010; 2(1): 36-40.

[27] Downing J. Effects of light absorption and scattering in water samples on OBS measurements. Campbell Scientific Inc; 2008, pp. 1-4.

[28] Ajibodu FA, Ojo BA. Performance Evaluation of the Maximum Achievable Bit Rate of a Next Generation TWDM Passive Optical Network. *American Journal of Engineering Research*, 2016; 5(1): 104-109.

Oluwabukola A. Ojediran obtained B. Tech degree in Electrical and Electronics Engineering from Ladoke Akintola University of Technology, Ogbomoso, Nigeria in 2007 and M. Sc in Electrical and Electronics Engineering (Communications) in 2015 at the University of Ibadan, Nigeria. She is currently on Ph.D. research in the Department of

Electrical and Electronics Engineering of the Federal University of Technology Akure, Nigeria. Her research interests are on biometrics and visible light communication system. She is a student member of Nigeria Society of Engineers (NSE), and a student member of Institute of Electrical and Electronics Engineers (IEEE).

Akinlolu A. Ponnle obtained B. Eng. and M. Eng. degrees in Electrical and Electronics Engineering (Communications) from The Federal University of Technology, Akure, Nigeria in 1998 and 2003 respectively. He obtained PhD degree (Electronics and Signal Processing) in 2011 from Tohoku University, Japan. His research interests include cardiovascular ultrasound imaging, signal processing, communication and electronics engineering, electromagnetic compatibility and wireless visible light communication. He currently teaches in the Department of Electrical and Electronics Engineering of the Federal University of Technology, Akure, Nigeria where he has been one time the Head of the Department. He is a member of Nigeria Society of Engineers (NSE), and a registered engineer with Council of Registered Engineers of Nigeria (COREN).

Samson A. Oyetunji obtained B. Eng. degree in Electrical and Electronics Engineering from University of Ilorin, Nigeria in 1988 and M. Eng. degree in Electrical and Electronics Engineering from University of Benin, Nigeria in 1994. He obtained PhD degree (Electronics and Communication) in 2012 from University of Benin, Nigeria. His research interests include signal processing, communication and electronics engineering, and wireless optical communication. He currently teaches in the Department of Electrical and Electronics Engineering of the Federal University of Technology, Akure, Nigeria where he has been one time the Head of the Department. He is a member of Nigeria Society of Engineers (NSE), and a registered engineer with Council of Registered Engineers of Nigeria (COREN).